Educational Administration: Theory and Practice
2024, 30(6),2706-2729
ISSN: 2148-2403
https://kuey.net/

Research Article

Study On Synthesis, Characterization And Medical Applications Of Zinc Nanoparticles In *T.Populnea*

Sara Palaparthy[1*], Prof. B.Sujatha[2]

[1*]Lecturer in Botany, Government Degree College, Ramachandrapuram, 533250
[2]Professor in Botany, Andhra University, Visakhapatnam, 530003

Citation: Sara Palaparthy, Prof. B.Sujatha, (2024) Study On Synthesis, Characterization And Medical Applications Of Zinc Nanoparticles In *T.Populnea Educational Administration: Theory And Practice*, *30* (6), 2706-2729
Doi: 10.53555/kuey.v30i6.5877

ARTICLEINO

ABSTRACT

Nanotechnology, spanning various disciplines, encompasses applications in science and technology, particularly in the manipulation of nanoparticles ranging from 1 to 100nm in size. The leaves and figs of the locally abundant *Thespesia populnea*, also known as the Portia tree, were selected for nanoparticle isolation in this study. For characterization, 0.1gm of each sample was mixed thoroughly with 1ml of dimethyl sulfoxide (DMSO) in separate tubes. Subsequently, 10µl of the prepared solution was analyzed using scanning electron microscopy (SEM) was conducted at magnifications ranging from500X to 80,800X, while X-ray diffraction (XRD) was performed at 2ɵ values between10–90 for characterization purposes. Antimicrobial activity assays involved loading sterilized nutrient agar and potato dextrose agar (PDA) with 100µl of Gram-positive bacteria, Gram-negative bacteria, and fungal organisms using the disc diffusion method. Zinc nanoparticles exhibited antibacterial activity against Gram-positive bacterium *Clostridium perfringens*, Gram-negative bacteria *Aeromonas hydrophila*, as well as fungi *Candida albicans*. These also shows antioxidant and antiproliferating activity.

Keywords: - Nanoparticles, Zinc oxide, DMSO, SEM, XRD, PDA, FTIR *Thespesia populnea*

1. INTRODUCTION: -

Nanotechnology encompasses the interdisciplinary study of particles ranging in size from 1 to 100 nanometers, exhibiting distinctive properties compared to their macroscopic counterparts. The documented applications of nanoparticles have broadened across diverse scientific fields such as food science, pharmaceuticals, healthcare, engineering, and notably agriculture (Wang et.,al) .These advancements stem primarily from progress in chemical synthesis techniques, which, in conjunction with alternative approaches, have the potential to enhance and accelerate nanoparticle manufacturing . Because of their heightened surface energy, nanoparticles demonstrate significant reactivity and thermodynamic instability, thus creating numerous motivations for synthesizing, advancing, and commercializing them (Lee et.,al 2023). Although nanoparticles present beneficial effects, concerns also arise regarding their potential toxicity to humans and plants. Nanoparticles typically exhibit unique physiochemical traits, including optical, thermal, and electrical properties, differing from those of bulk particles. Typically, the synthesis of nanoparticles involves integrating reducing or precipitating agents into their construction process. (Fan Z et.,al 2005).The development of green synthesis methods for nanomaterials, excluding harmful chemicals, has become a significant focal point in nanoscience research, driving the progress of environmentally sustainable methodologies (Kalpana et.,al *2018*,). Plant-mediated nanoparticle synthesis, a form of green synthesis, has emerged as a viable alternative to physical and chemical approaches. Unlike traditional methods, it presents a direct and rapid process utilizing safer and eco-friendly substances. Furthermore, aside from addressing environmental concerns such as solar interaction, catalysis, and agricultural yield, green synthesis contributes to the production of renewable energy (Liu et.,al 2023)**.** Various plants, including Aloe Vera, Punica granatum, and Allium sativum, have been utilized for the synthesis of Zinc nanoparticles. While environmentally friendly synthesis techniques for nanoparticles are abundant, only a limited number have been applied to Zinc synthesis. The use of green methods for Zinc nanoparticle synthesis is favored due to their environmental benefits, avoiding the need for specific chemical stabilizers and reducers, and enabling preparation under mild ambient conditions .In biological synthesis of Zinc nanoparticles, raw materials such as plant extracts, microbes, and fungi are employed, allowing for control

over shape and size. Characterization techniques such as UV-Vis spectroscopy and X-ray diffraction (XRD) are commonly used to confirm the formation and determine the crystalline structure of Zinc nanoparticles .Similar to Zinc, various plants have been employed for the synthesis of Iron nanoparticles. The utilization of environmentally friendly methods for Iron nanoparticle synthesis is preferred due to their advantages in terms of biocompatibility and ease of preparation (Nomal et.,al). Biological synthesis methods involving plant extracts, microbes, and fungi are commonly used for the fabrication of Iron nanoparticles, offering control over their properties. Characterization techniques such as XRD and SEM are used to analyze the shape, size, and crystalline structure of Iron nanoparticles (Jin et.,al). Iron nanoparticles have gained attention for their potential applications in fields such as bio sensing, drug delivery, and environmental remediation.

2. Materials & Methods:

2.1 Materials: -

Leaves and figs of the ***Thespesia populnea*** tree, DMSO (Dimethyl Sulfoxide), ZnO, Nutrient agar media, Ethanol, Potato Dextrose agar, Double distilled water, PH Meter

Synthesis of Zinc Oxide Nanoparticles:

For the preparation of Zinc Oxide nanoparticles, 4 grams of Zinc Sulphate heptahydrate is dissolved in 100 mL of leaf, fruit and stem extracts each, in 3 different flasks. Then, the pH of the mixture was adjusted to 7.0, by the drop-wise addition of 0.02 M aqueous NaOH solution. The solutions are then heated over a water bath for 2 hours at 60°C. The solutions are then centrifuged for 10 minutes at 4000rpm. The supernatant is discarded and the nanoparticles (pellet) are collected and dried in a hot air oven (Bahrulolum et.,al 2021).

Characterization

UV Visible:-

Eppendorf tubes are labeled with specific parameters for each Nanoparticle, and 0.1gm of Zn NPs are mixed with DMSO in each tube. Subsequently, 10µl of the resulting sample is transferred into quartz cuvettes, followed by the addition of 1ml of distilled water and thorough mixing. Readings are then obtained using a UV-Visible spectrophotometer within the range of 200-600nm. UV-Vis spectroscopy proves to be invaluable for identification, as unique peaks emerge at distinct wavelengths of light owing to the presence of SRP electrons on NP surfaces. Zn NPs' optical properties and concentrations are determined utilizing UV-Vis spectroscopy (Somu et.,al 2022).

SEM Analysis of Zn NP's:-

The Scanning Electron Microscope (SEM) was utilized to capture morphological images across a diverse array of samples, offering magnification ranging from 500X to 80,800X. The microphotographs of nanocomposites emerged under the influence of high-energy electron beams. Through the interaction between electrons and sample atoms, signals are generated, revealing the composition and surface morphology of the synthesized nanocomposites. SEM boasts resolutions finer than a nanometer and allows specimen observation even in wet conditions. By detecting scattered electrons, SEM provides comprehensive insights into the surface morphology of the sample (Hall et.,al 2007).

XRD Analysis of Zn NP's:-

Utilizing Zn Kα (λ =1.540 ˚ A) as the radiation source, a crystallographic analyzer facilitated the examination of Cu NPs with a scan speed of 0.4°/min and a 2θ range spanning 10–90. Through XRD analysis, the compound's crystal structure and chemical composition were successfully determined. Additionally, X-ray energy-dispersive spectroscopy was employed to evaluate the chemistry of the nanoparticles (Zhang et.,al 2022).

FTIR Analysis of Zn NP's:-

The bonding characteristics of the thick films were assessed by Fourier-transform infrared spectrometer (FTIR), scanning from 500 to 4000 cm-1 at a resolution of 2 cm-1. This analysis aimed to ascertain the presence of functional groups within the synthesized ZnO NPs (Alarifi et al 2019).

Anti-bacterial activity of Zn nanoparticles:

The Nutrient agar media preparation began by adding 1.3gms of nutrients to 100ml of distilled water in a conical flask, ensuring thorough mixing, followed by the addition of 2gms of agar. A cotton plug was then placed at the mouth of the conical flask to cover it. Petri dishes were meticulously cleaned with ethanol and securely packed. The media and plates underwent sterilization in an autoclave at 121°C temperature and 15lbs pressure for 15 minutes. Once solidified, 100µl of microorganisms were evenly spread on the plates using an L-shaped rod, and wells were created with a cork borer. Subsequently, 10µl of respective Zn nanoparticle solutions were loaded into the designated wells. The plates were then incubated at 37°C to promote microbial growth, and the antibacterial activity was evaluated by observing and measuring the zones of inhibition around each well. This assessment encompassed five gram-negative bacteria*: Bacillus subtilis, Bacillus licheniformis, Clostridium*

perfringens, Staphylococcus epidermidis, and Staphylococcus aureus, as well as five gram-positive bacteria: *Aeromonas hydrophila, Vibrio cholera, Escherichia coli, Pseudomonas aeruginosa, and Salmonella enterica*(Mendes et.,al 2022).

Anti-fungal activity of Zn nanoparticles:

The preparation of Potato Dextrose Agar Nutrient media commenced by combining 100ml of distilled water with 1.3gms of nutrient in a conical flask, ensuring thorough mixing before adding 2gms of agar and mixing again. A cotton plug was fashioned to cover the flask's mouth. Petri dishes underwent meticulous cleaning with ethanol before being securely packed. The media and plates underwent sterilization in an autoclave at 121℃ and 15lbs pressure for 15 minutes, after which the autoclave was turned off upon reaching the specified pressure. Subsequently, the media and plates were transferred to a cleaned laminar airflow hood. Once opened, the media was poured into the plates and allowed to solidify for 10 to 15 minutes before closing the plates. Following solidification, 100µl of microorganisms were evenly spread on the plates using an L-shaped rod, and wells were created with a cork borer, each labeled with sample numbers. Ten microliters of respective Zn nanoparticle solutions were loaded into the designated wells. The plates were then incubated at 37℃ to promote microbial growth, and the anti-fungal activity was assessed by observing and measuring the zones of inhibition around each well. This assessment encompassed five fungal organisms: *Aspergillus niger, Aspergillus flavus, Candida albicans, Saccharomyces cerevisiae, and Phytophthora infestans* (Abomuti et,al 2021; Xu et.,al 2021)

Results:-

Characterization
U.V.Visible:-

Zn stem

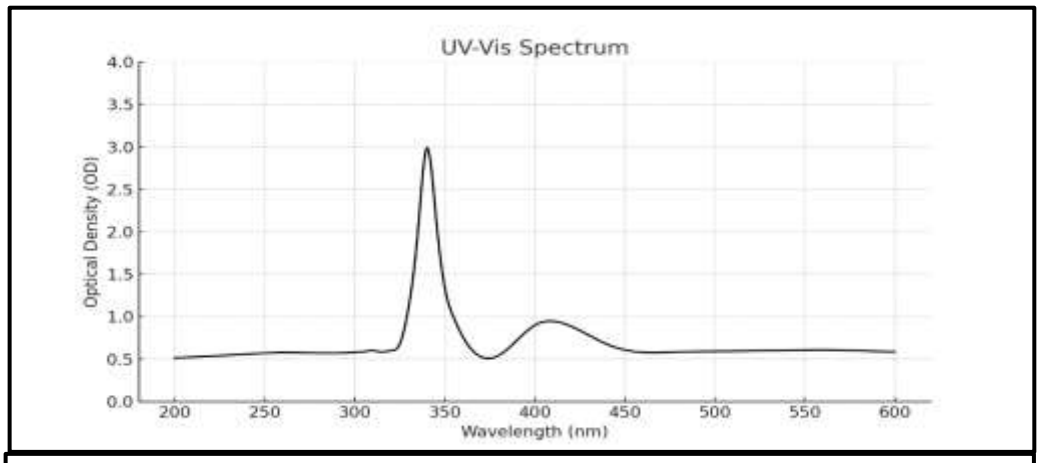

GRAPH 1- In the above graph high optical density is observed at 348nm

Zn Leaf

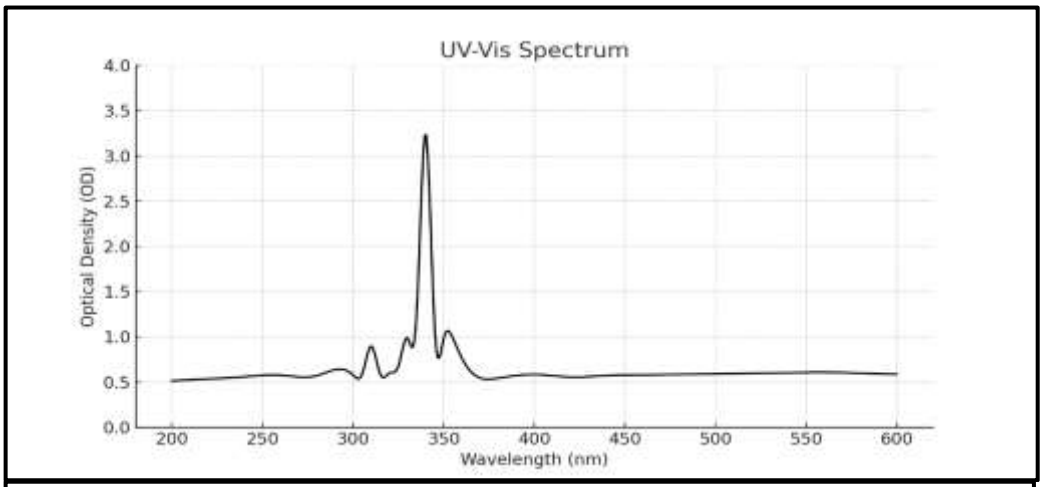

GRAPH 2- In the above graph high optical density is observed at

Zn fruit

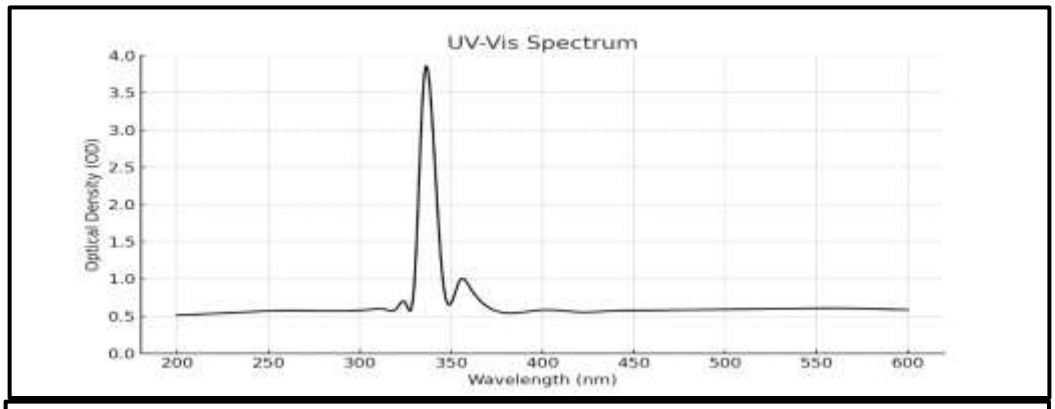

GRAPH 3- In the above graph high optical density is observed at 348nm

SEM Analysis

Zn stem

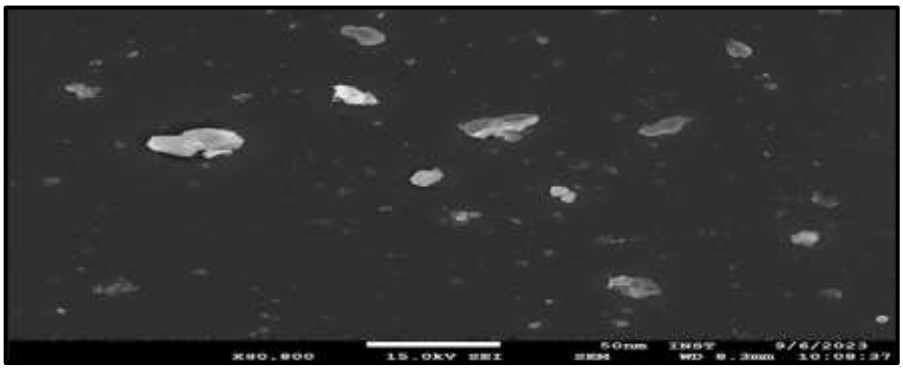

Zn leaf

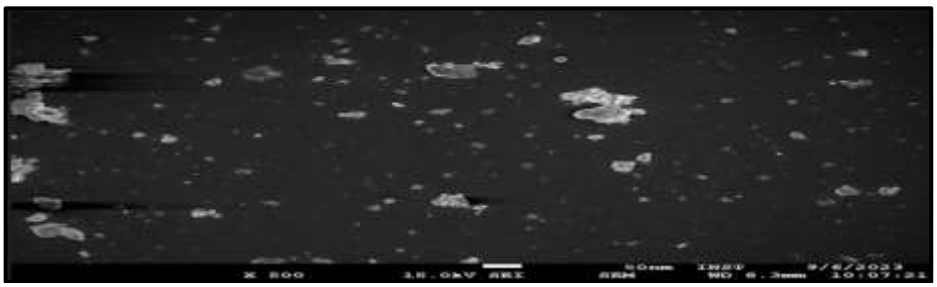

Zn fruit

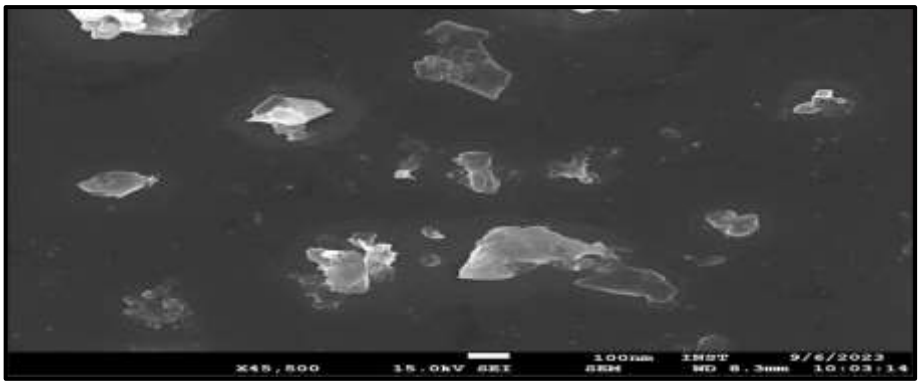

Morphology and the size of the Zn NPs were detected using the Scanning Electron Microscope (SEM). It is concluded from given figures that the particles in the samples were compactly arranged and were almost spherical in shape. However, the study shows the size range is 20 nm - 120µm, with an average size of 64 nm.

XRD Analysis
Zn Stem

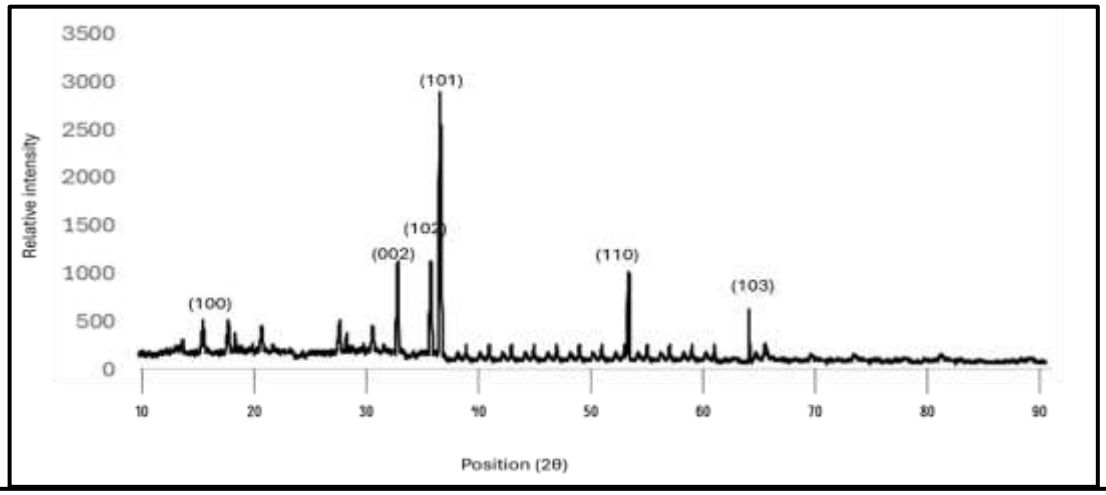

GRAPH 6- XRD Pattern of synthesized Zn Nanoparticle using *T.populnea* stem extract highest peak is observed t 2ɵ = 37^0

Zn Leaf
Zn fruit

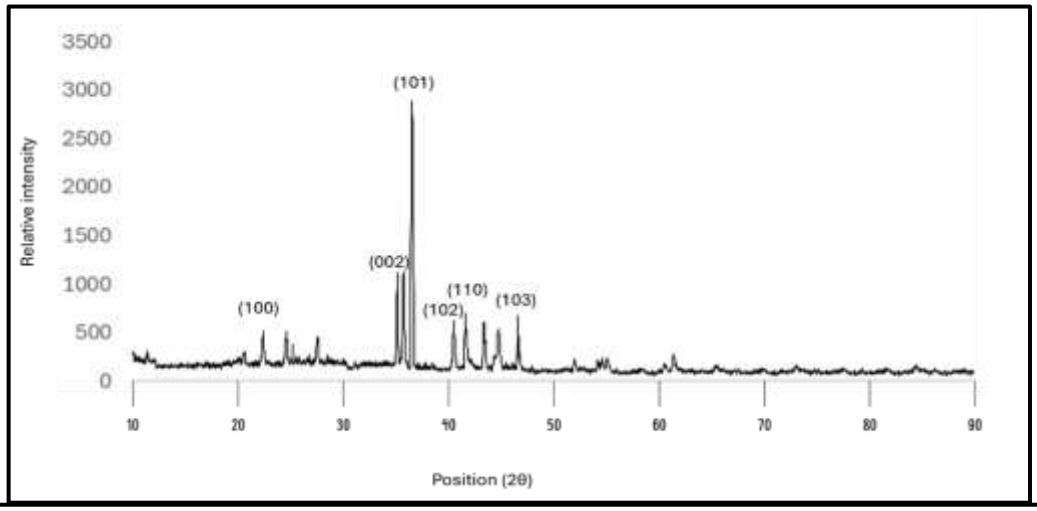

GRAPH 5 - XRD Pattern of synthesized Zn Nanoparticle using *T.populnea* leaf extract highest peak The highest peak is observed at 2ɵ = 37^0

FTIR Analysis
Zn Stem

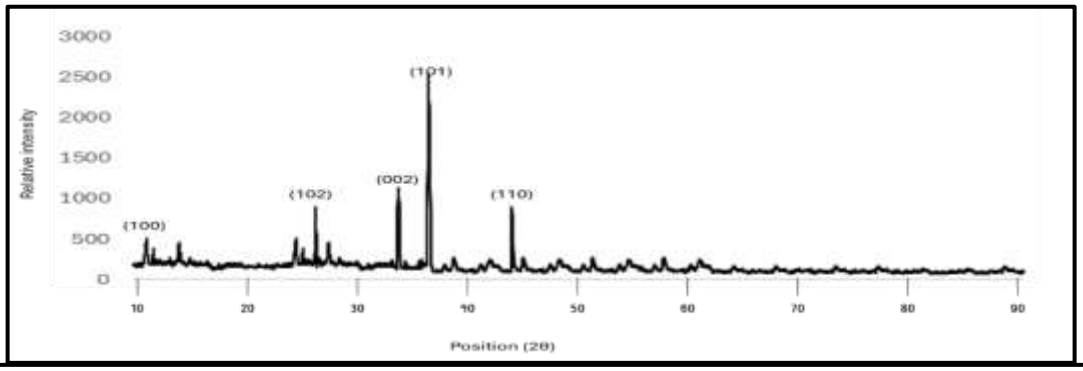

GRAPH 4 - XRD Pattern of synthesized Zn Nanoparticle using *T.populnea* fruit extract highest peak is observed t 2ɵ = 37^0

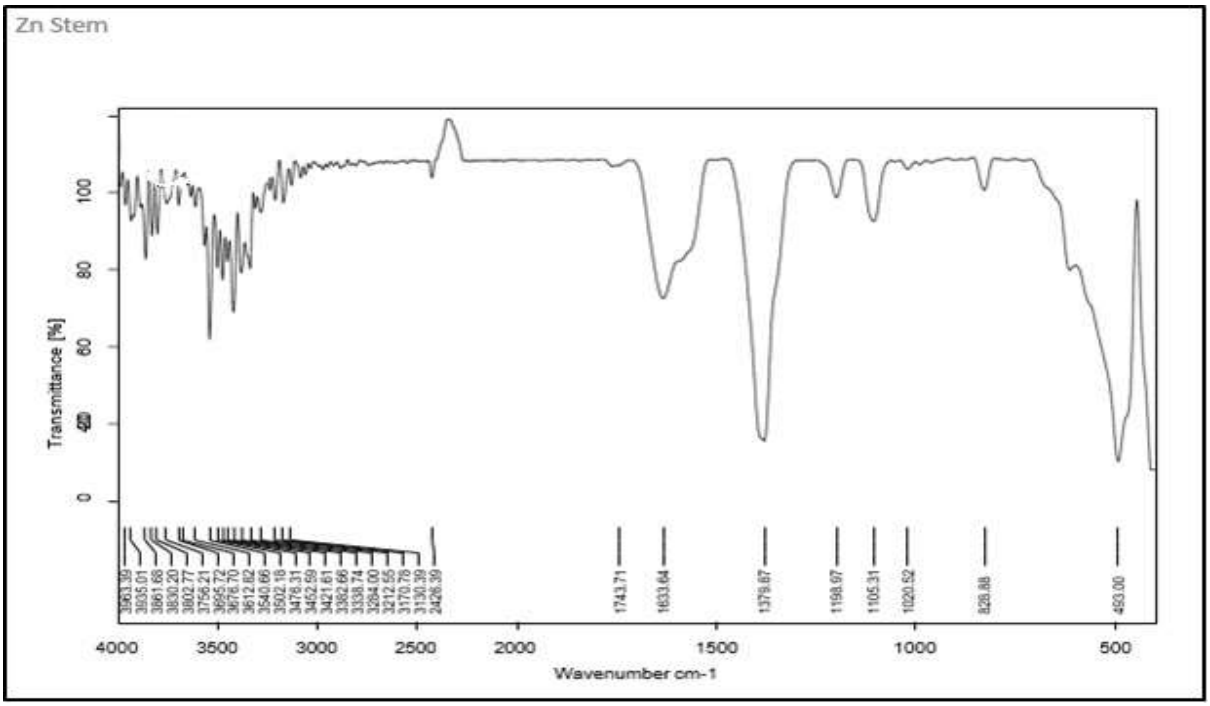

432, 457 cm^{-1} : Zn-O stretching, characteristic of zinc oxide formations.
483, 617 cm^{-1} : Further Zn-O vibrations or interactions with organic cappings.
828, 835 cm^{-1} : Suggestive of organic molecule interactions or out-of-plane aromatic C-H bends.
1020, 1112 cm^{-1} : C-O stretching, typical in organic ethers or esters.
1195, 1198 cm^{-1} : C-N stretching, indicating the presence of amines.
1379, 1384 cm^{-1} : C-H bending, possibly from organic ligands.
1627, 1772 cm^{-1} : Amide I bands or C=C stretching, suggesting complex organic modifications.
2424, 3402 cm^{-1} : Possible CO_2 or triple-bond stretches.
3452, 3528 cm^{-1} : Broad O-H stretching from hydroxyl groups or water molecules.

Zn Leaf

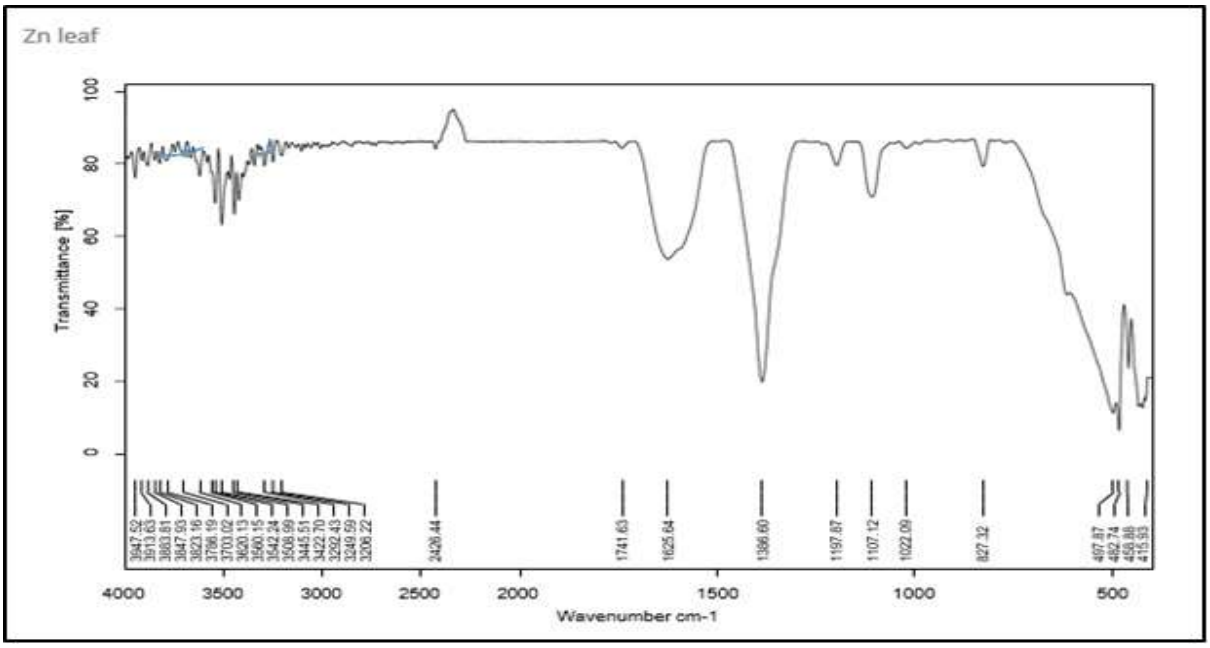

457, 483 cm^{-1} : Zn-O stretching vibrations, typical of zinc oxide.
617, 835 cm^{-1} : C-H out-of-plane bends or Si-O stretching.
828, 1022 cm^{-1} : C-O stretching in ethers or esters, indicating organic coatings.
1105, 1198 cm^{-1} : C-N stretching in amines or complex ring structures.

1379, 1384 cm^{-1} : C-H bending vibrations, possibly from methyl groups.
1627, 1772 cm^{-1} : Amide bands or C=C stretching vibrations in unsaturated carbonyl compounds.
2424, 3402 cm^{-1} : High wavenumber peaks often from multiple bonded or absorbed atmosphericgases like CO_2.
3452, 3528, 3540 cm^{-1} : Broad O-H stretch vibrations indicating hydrogen bonding or absorbed moisture.

Zn Fruit

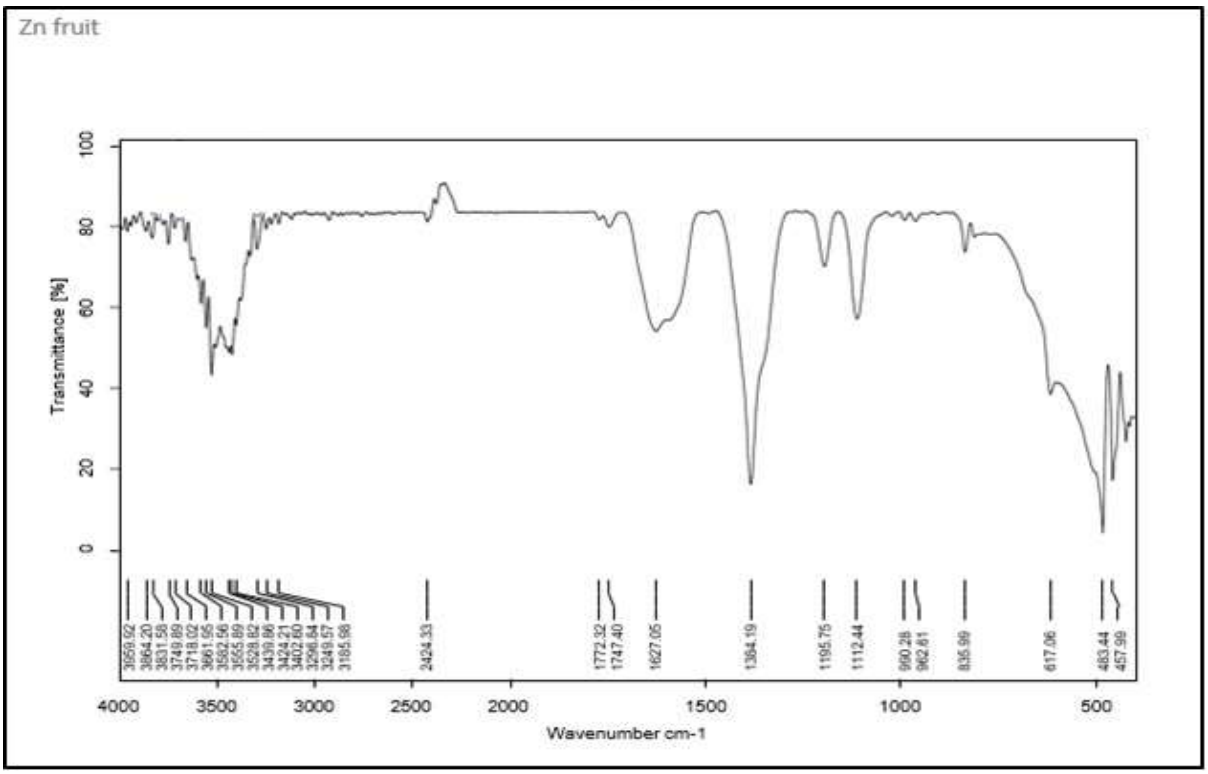

432, 457 cm^{-1} : Indicative of Zn-O stretching vibrations, showing zinc oxide presence.
483, 617 cm^{-1} : Further evidence of Zn-O interactions, possibly with organic coatings.
828, 835 cm^{-1} : Organic interactions or C-H out-of-plane bends in aromatic rings.
1022, 1112 cm^{-1} : C-O stretching in ethers or esters, showing organic surface modifications.
1195, 1198 cm^{-1} : C-N stretching vibrations, likely amines or nitriles.
1379, 1384 cm^{-1} : C-H bending vibrations from organic coatings.
1627, 1772 cm^{-1} : Amide bands or C=C stretching in unsaturated compounds.
2424, 3402 cm^{-1} : High wavenumber peaks from atmospheric adsorption or multiple bondedsystems.
3452, 3528 cm^{-1} : Broad O-H stretching, indicative of hydrogen bonding or moisture.

Antimicrobial activities

Effect of Zinc Nano Particle on gram positive bacteria

S.No	organism	Stem			Leaf			Fruit		
		100 µg	250 µg	500 µg	100 µg	250 µg	500 µg	100 µg	250 µg	500 µg
1	*Bacillus subtilis*	8	8	10	10	12	16	7	9	12
2	*Bacillus licheniformis*	10	11	13	10	11	16	8	10	11
3	*Clostridium perfringens*	12	14	16	15	20	**25**	10	12	15
4	*Staphylococcus epidermidis*	10	11	14	12	14	17	10	12	13
5	*Staphylococcus aureus*	8	10	14	13	15	18	0	9	12

Effect of Zinc Nano particle on gram negative bacteria

S.No	organism	Stem			Leaf			Fruit		
		100 µg	250 µg	500 µg	100 µg	250 µg	500 µg	100 µg	250 µg	500 µg

1	*Aeromonas hydrophila*	10	13	15	13	16	**21**	8	11	8
2	*vibrio cholera*	0	0	8	10	12	15	8	8	12
3	*Escherichia coli*	0	8	11	10	10	11	8	8	10
4	*pseudomonas aeruginosa*	8	10	11	10	11	13	8	12	13
5	*salmonella enterica*	8	9	13	12	14	16	8	12	15

Effect of Zinc Nano particle on Fungi

S.No	Organism	Stem			Leaf			Fruit		
		100 µg	250 µg	500 µg	100 µg	250 µg	500 µg	100 µg	250 µg	500 µg
1	*Aspergillus niger*	0	0	8	0	0	0	0	8	8
2	*Aspergillus flavus*	0	0	0	0	0	9	0	0	8
3	*Candida albicans*	0	10	13	10	11	**16**	8	11	14
4	*saccharomyces cerevisiae*	0	0	8	0	8	8	0	0	9
5	*phytophthora infestans*	8	9	9	10	10	13	8	10	13

1. Bacillus subtilis

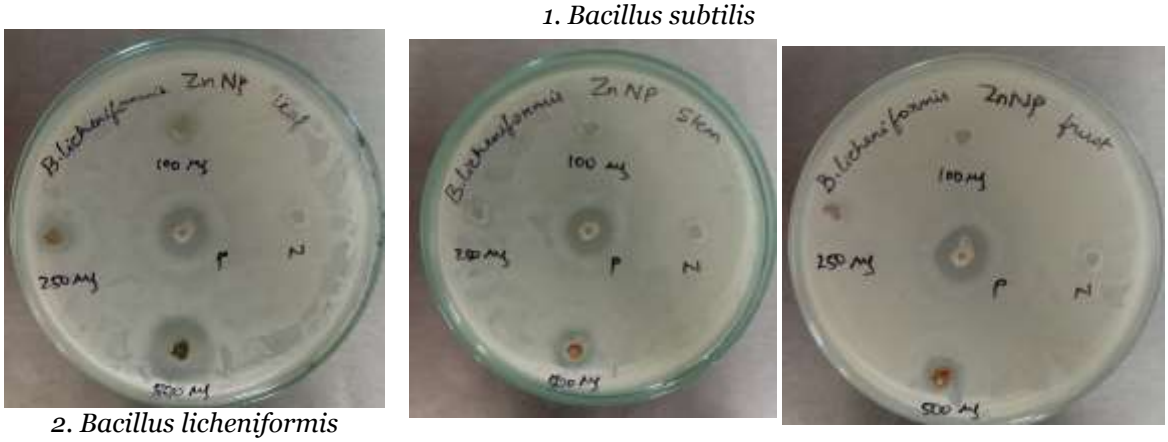

2. Bacillus licheniformis

3. Clostridium perfringens

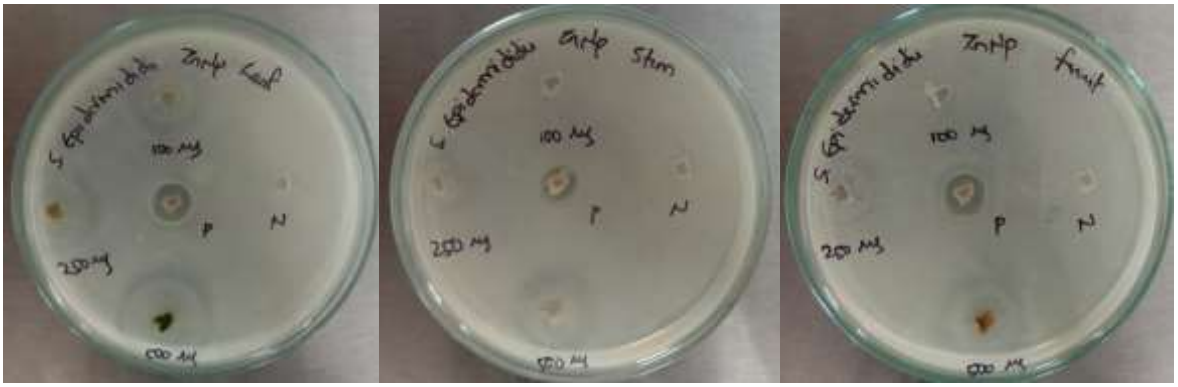

4. Staphylococcus epidermidis

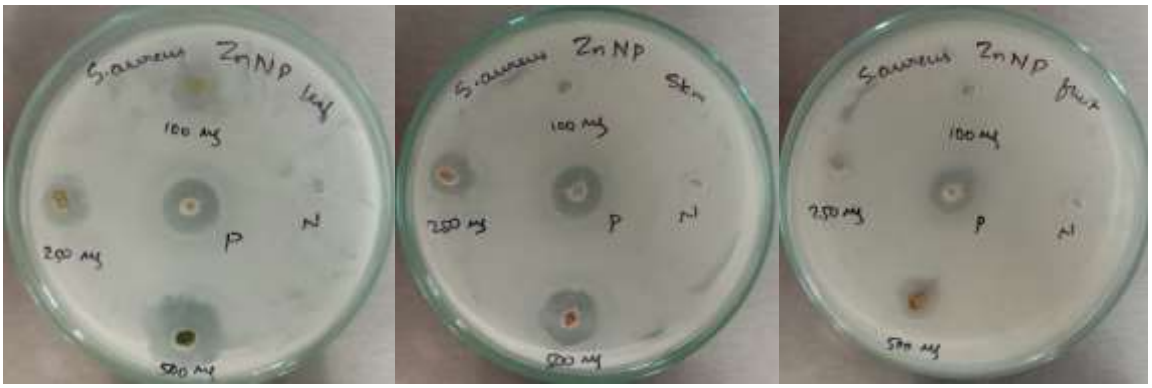

5. Staphylococcus aureus

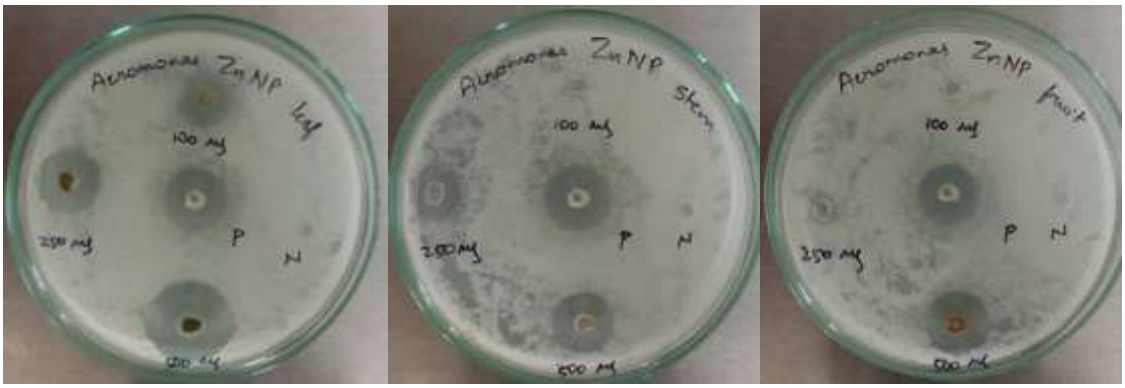

6. Aeromonas hydrophila

7. vibrio cholera

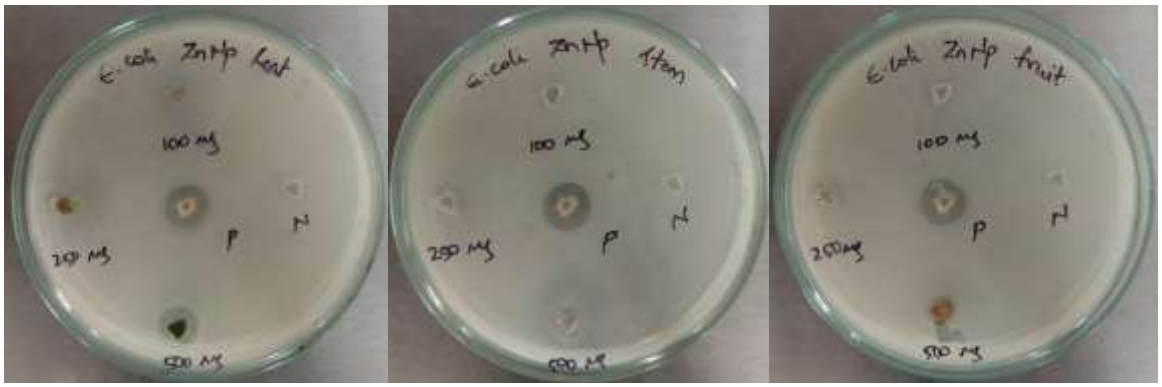

8. Escherichia coli

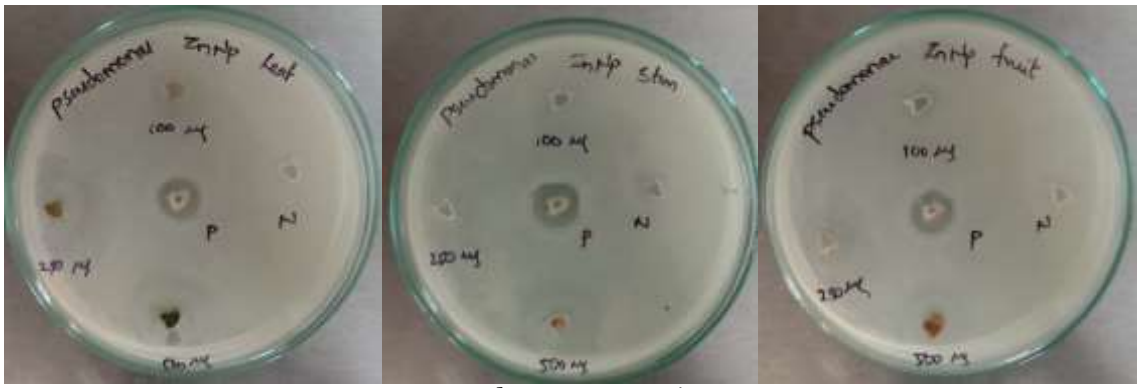

9. Pseudomonas aeruginosa

10. Salmonella enterica

11. Aspergillus flavus

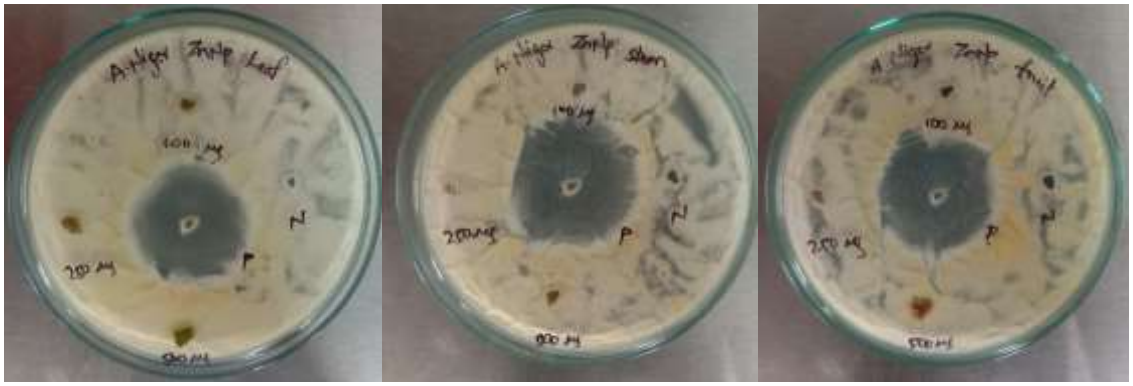

12. Aspergillus niger

13. Candida albicans

14. Phytophthora infestans

15. Saccharomyces cerevisiae

Evaluation of antioxidant activity by DPPH radical scavenging method

Free radical scavenging activity of different chemical compounds were evaluated. In brief, 0.1 mM solution of DPPH in ethanol was prepared. This solution (1 ml) was added to 3 ml of different compounds in ethanol at different concentration (200, 400, 600, 800 and 100 µg/ml). The mixture was shaken vigorously and allowed to stand at room temp for 30 min. then, absorbance was measured at 517 nm by using spectrophotometer (UV-VIS Shimadzu). Reference standard compound being used was ascorbic acid and experiment was done in triplicates. Lower absorbance of the reaction mixture indicated higher free radical activity. Ascorbic acid at various concentrations (20 to 100 µg/ml) was used as standard (Kalaimurugan et.,al ; Asif et.,al) .The percent DPPH scavenging effect was calculated by using following equation.

DPPH scavenging effect (%) or Percent inhibition = A0 - A 1 / A0 × 100.

Where

A0 was the Absorbance of control reaction and

A1 was the Absorbance in presence of test or standard sample.

Zn Stem

	Concentration (µg)	Od	Percent reduction
Zn stem	62.5	2.34	21.48
	125	2.18	26.85
	250	1.62	45.64
	500	1.15	61.41
	1000	0.99	66.78

		IC 50	505.47

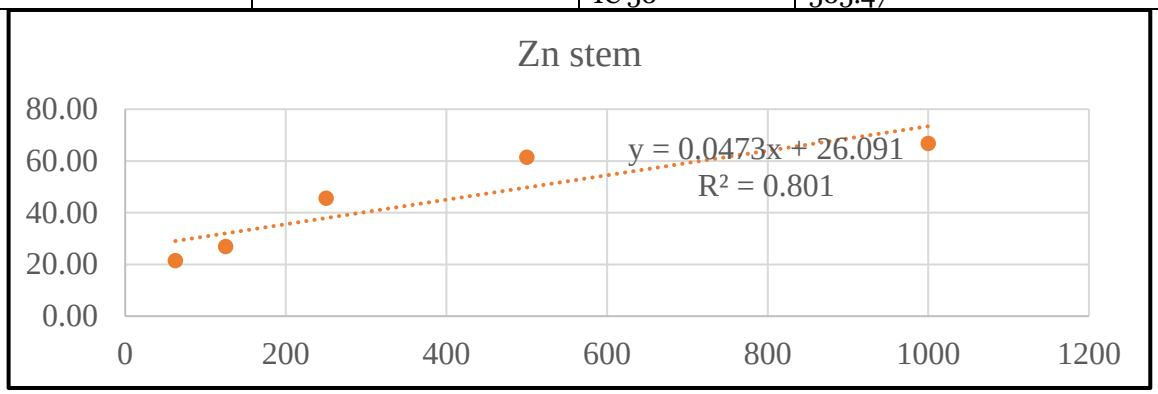

Zn Leaf

	Concentration (µg)	Od	Percent reduction
Zn leaf	62.5	2.19	26.51
	125	2.04	31.54
	250	1.83	38.59
	500	1.37	54.03
	1000	0.86	71.14
		IC 50	507.13

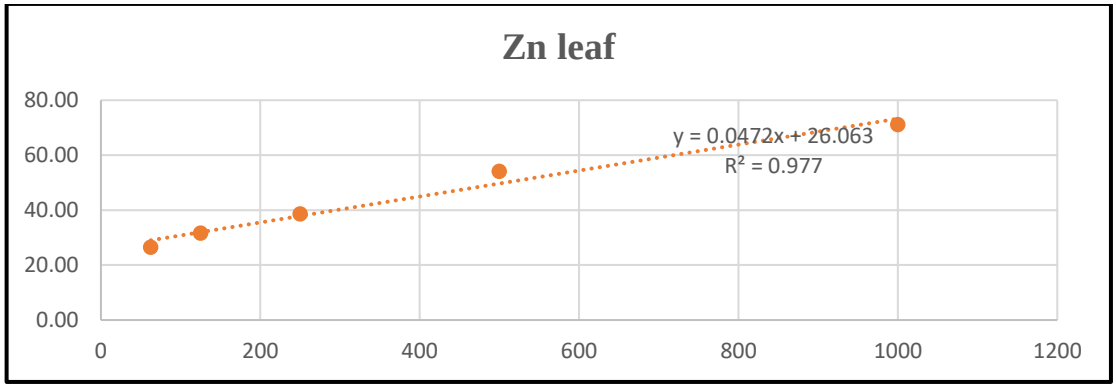

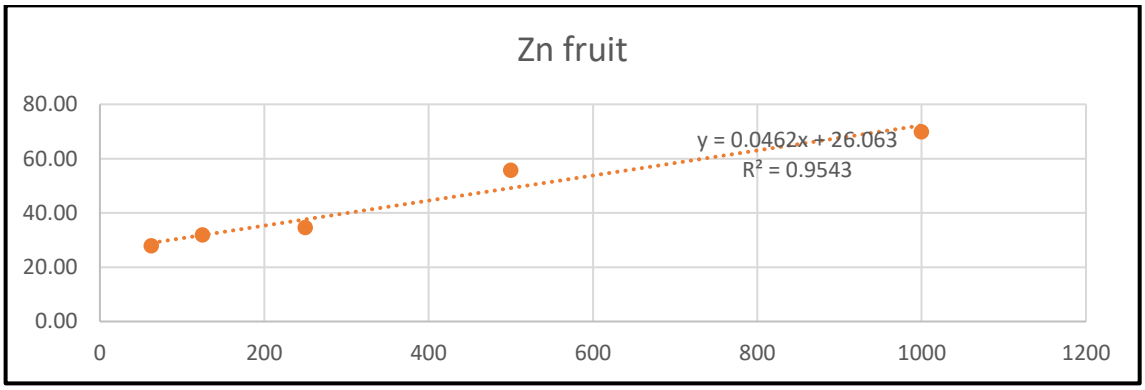

Zn Fruit

	Concentration (µg)	Od	Percent reduction
Zn Fruit	62.5	2.15	27.85
	125	2.03	31.88
	250	1.95	34.56
	500	1.32	55.70
	1000	0.9	69.80
		IC 50	518.11

FRAP assay

The assay was carried out for different extracts as demonstrated by Lim et al. (2013) with slight modifications. Three hundred millimolar of acetate buffer (pH 3.6), 20 mM TPTZ solution (40 mM HCl) and 20 mM FeCl3

(Water) were mixed together in the ratio of 10:1:1 to make FRAP solution and tested against extracts by allowing it to react with the FRAP solution in the ratio of 1:30 for 30 min in dark at 37°C. The blue colored product (Ferrous tripyridyltriazine complex) was formed and absorbance was taken at 593nm spectrophotometrically. Ascorbic acid at various concentrations (20 to 100µg/ml) was used as standard.

Zn stem

compound	Concentration (µg)	Od	percent reduction
Zn stem	62.5	1.43	21.90
	125	1.15	37.19
	250	0.94	48.66
	500	0.72	60.68
	1000	0.66	63.95
		IC 50	478.60

Zn leaf

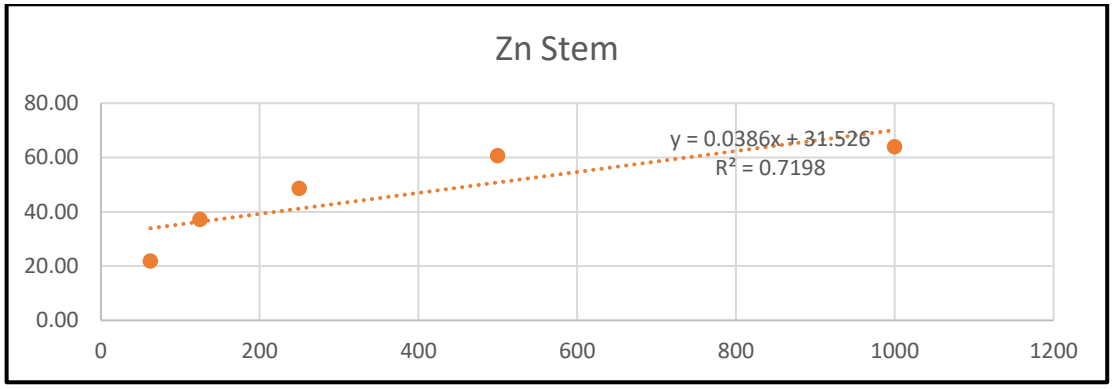

compound	Concentration (µg)	Od	percent reduction
Zn leaf	62.5	1.52	16.99
	125	1.28	30.09
	250	0.9	50.85
	500	0.84	54.12
	1000	0.69	62.32
		IC 50	561.58

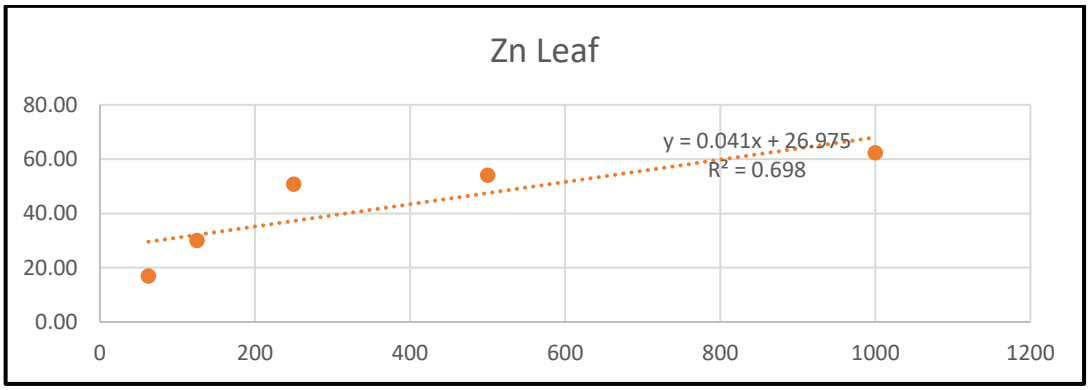

Zn Fruit

compound	Concentration (µg)	Od	percent reduction
Zn Fruit	62.5	1.37	25.18
	125	1.01	44.84
	250	0.86	53.03
	500	0.69	62.32
	1000	0.53	71.05
		IC 50	355.13

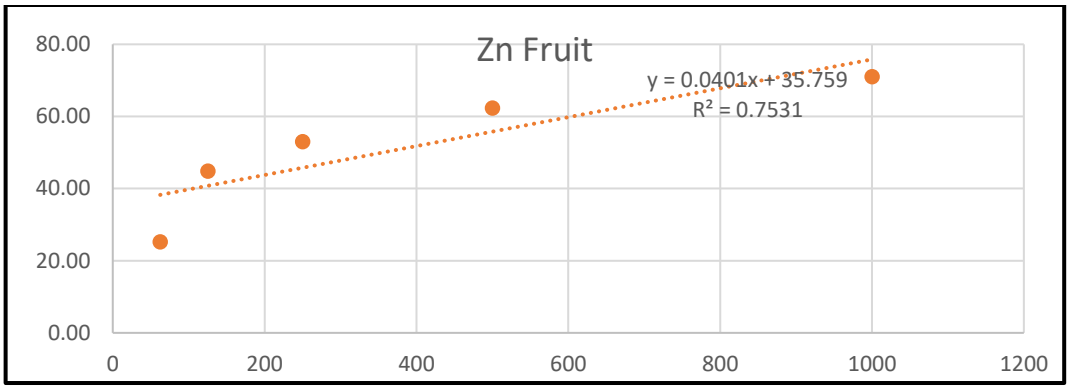

H_2O_2 Scavenging Activity

Scavenging activity of hydrogen peroxide by the plant extract was estimated using the method of Ruch *et al.*(1989) with little modification. 4 mmol/L solution of H_2O_2 was prepared in PBS (pH 7.4). Plant extract (4 mL), prepared in distilled water at various concentration was mixed with 0.6 mL of 4 mmol/L H_2O_2 solution prepared in PBS and incubated for 10 min. The absorbance of the solution was taken at 230 nm against a blank solution containing the plant extract in PBS without H_2O_2. Ascorbic acid was used as positive control. The amount of hydrogen peroxide radical inhibited by the extract was calculated using the following equation:

H_2O_2 radical scavenging activity=$(A_{control}-A_{test})/A_{control}\times 100$

Where $A_{control}$ is the absorbance of H_2O_2 radical+methanol; A_{test} is the absorbance of H_2O_2 radical+sample extract or standard.

compound	Concentration (µg)	Od	percent reduction
Zn stem	62.5	1.36	25.27
	125	1.19	34.62
	250	0.96	47.25
	500	0.73	59.89
	1000	0.54	70.33
		IC 50	443.57

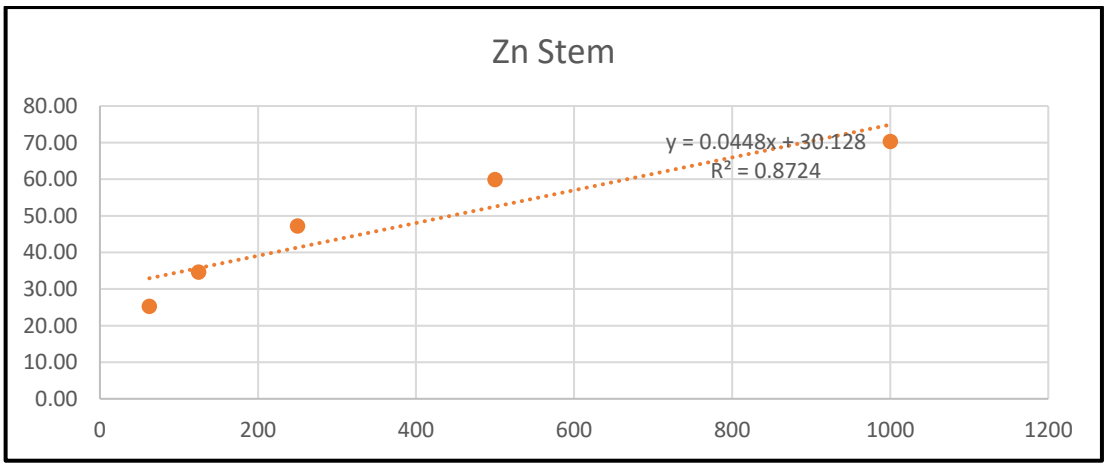

compound	Concentration (µg)	Od	percent reduction
Zn leaf	62.5	1.48	18.68
	125	1.31	28.02
	250	0.99	45.60
	500	0.78	57.14
	1000	0.51	71.98
		IC 50	495.45

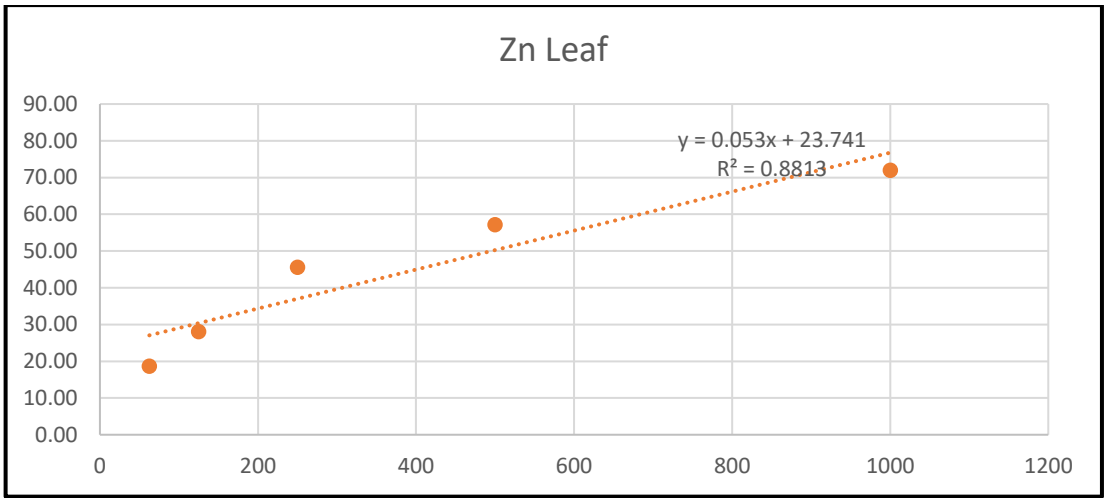

compound	Concentration (µg)	Od	percent reduction
Zn Fruit	62.5	1.38	24.18
	125	1.14	37.36
	250	0.96	47.25
	500	0.65	64.29
	1000	0.43	76.37
		IC 50	389.28

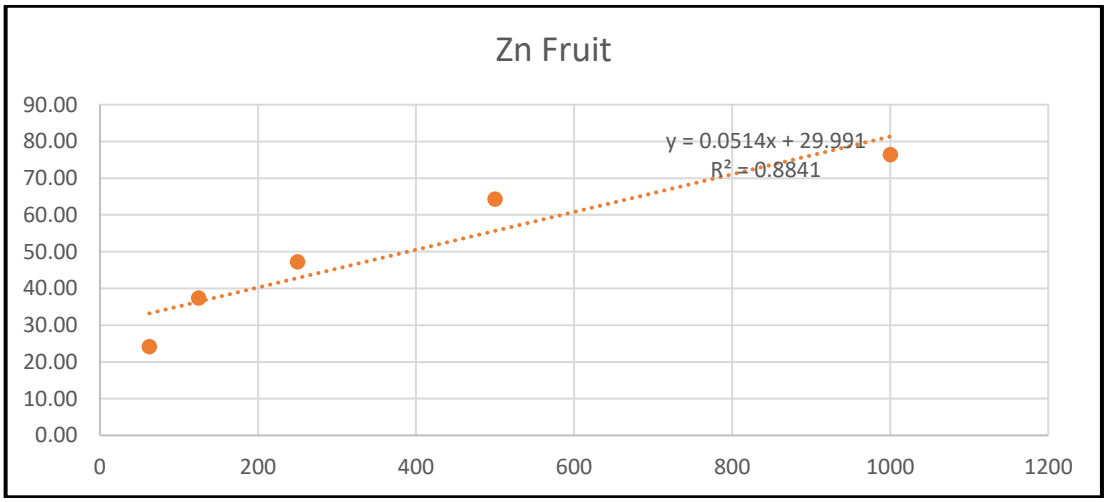

In vitro anti-inflammatory activity

Inhibition of albumin denaturation

Methods of Mizushima and Kobayashi were followed with minor modifications. The reaction mixture was consisting of test extracts and 1% aqueous solution of bovine albumin fraction, pH of the reaction mixture was adjusted using a small amount at 37°C Hcl. The sample extracts were incubated at 37°C for 20 min and then heated to 51°C for 20 min after cooling the samples the turbidity was measured spectrophotometrically at 660 nm. The experiment was performed in triplicate. Percent inhibition of protein denaturation was calculated as follows,

% inhibition= [{Abs control- Abs sample}/Abs control] x 100,

Where, Abs control is the absorbance without sample, Abs sample is the absorbance of sample extract/standard.

	Conc (µg/ml)	OD	Percent inhibition
Zn stem	62.5	1.49	30.37
	125	1.28	40.19
	250	1.04	51.40
	500	0.99	53.74
	1000	0.83	61.21

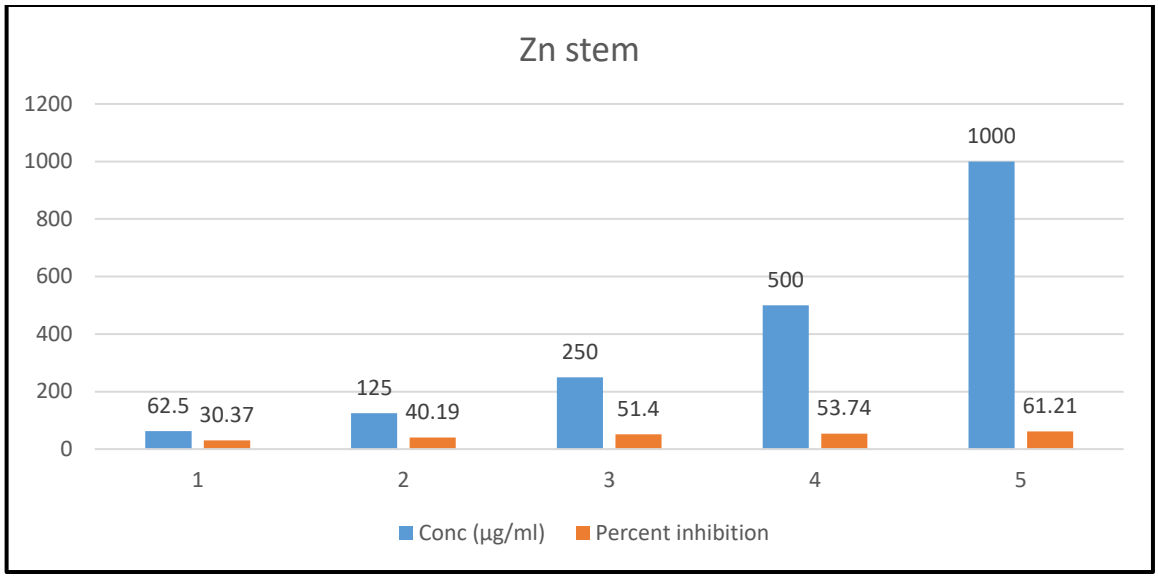

	Conc (µg/ml)	OD	Percent inhibition
Zn leaf	62.5	1.45	32.24
	125	1.19	44.39
	250	1.03	51.87
	500	0.97	54.67
	1000	0.74	65.42

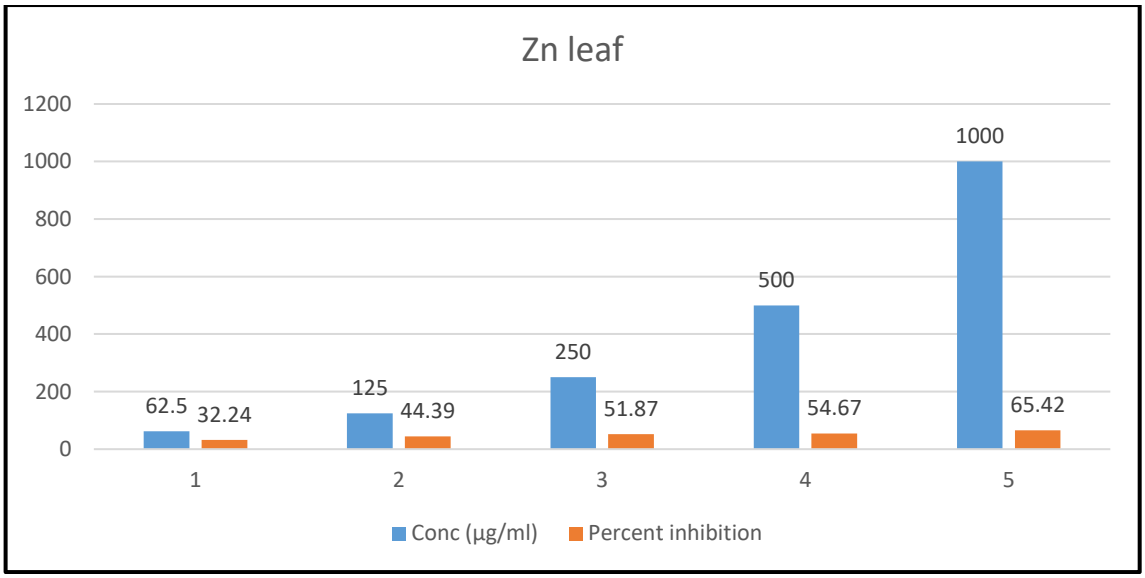

	Conc (µg/ml)	OD	Percent inhibition
Zn fruit	62.5	1.38	35.51
	125	1.02	52.34
	250	0.84	60.75
	500	0.72	66.36
	1000	0.53	75.23

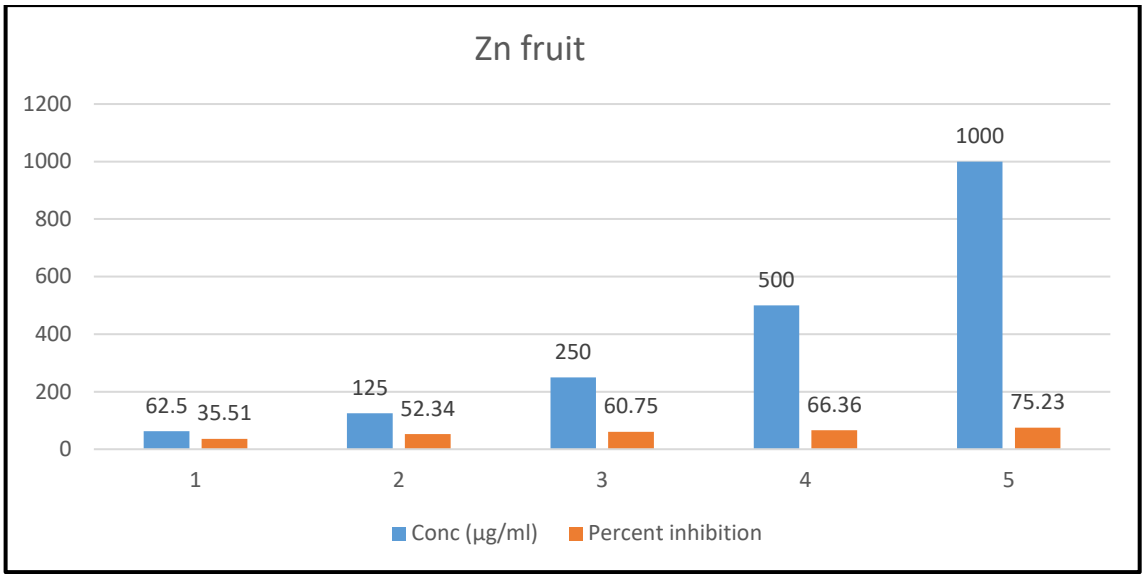

Membrane stabilization test

Preparation of red blood cells (RBCs) suspension

Fresh whole human blood (10 ml) was collected and transferred to the centrifuge tubes. The tubes were centrifuged at 3000 rpm for 10min and were washed three times with equal volume of normal saline. The volume of blood was measured and reconstituted as 10% v/v suspension with normal saline

Hemolytic activity

The hemolysis assay was determined according to Slowing et al. (2009) with some modifications. Human blood type A cells were obtained from Centro de Hematologia e Hemoterapia do Ceará (HEMOCE) and prepared by washing them six times with 50 Mm Tris-HCl, pH 7.6, containing NaCl 0.15 M (TBS). Following the last wash, red blood cells (RBC) were diluted to 1/10 of their volume with TBS. The assay was performed by mixing 0.3 mL of the RBC solution with 1.2 mL of 70% EtOH crude extract and DMC, EtOAc and Aq fractions (12.5, 25, 50, and 100 µg mL-1); 1.2 mL of distilled water was set as a positive control and 1.2 mL of TBS as a negative control. The mixtures were vortexed, left for 2 h at room temperature, and then centrifuged at 4,000 x g for 10 min at 4°C. Absorbance of the supernatants was measured at 541 nm in a UV-Vis spectrophotometer. The percentage of hemolysis of each fraction was calculated using the expression below:

Hemolytic activity = Abs sample–Abs negative control/ Abs positive control – Abs negative control X 100

	Conc (µg/ml)	OD	Percent inhibition
Zn stem	**62.5**	**1.428**	**0.18**
	125	**1.415**	**1.32**
	250	**1.395**	**3.07**
	500	**1.378**	**4.56**
	1000	**1.339**	**7.98**

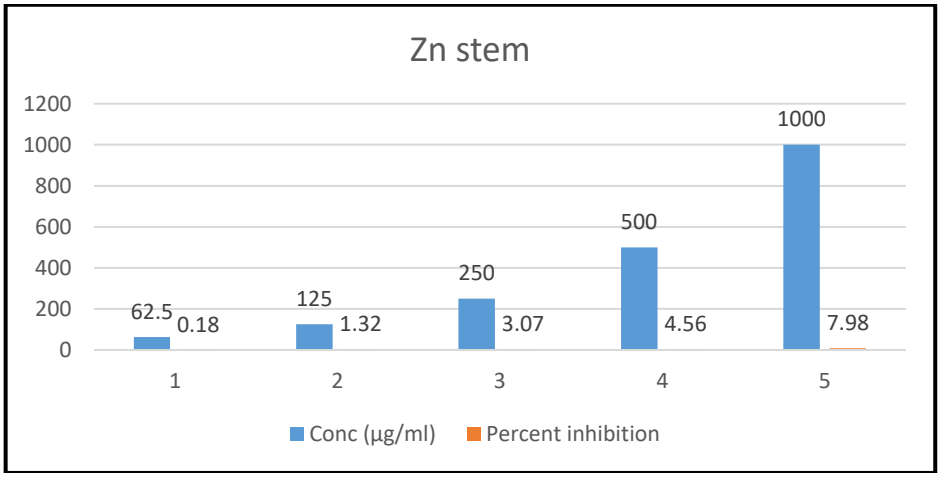

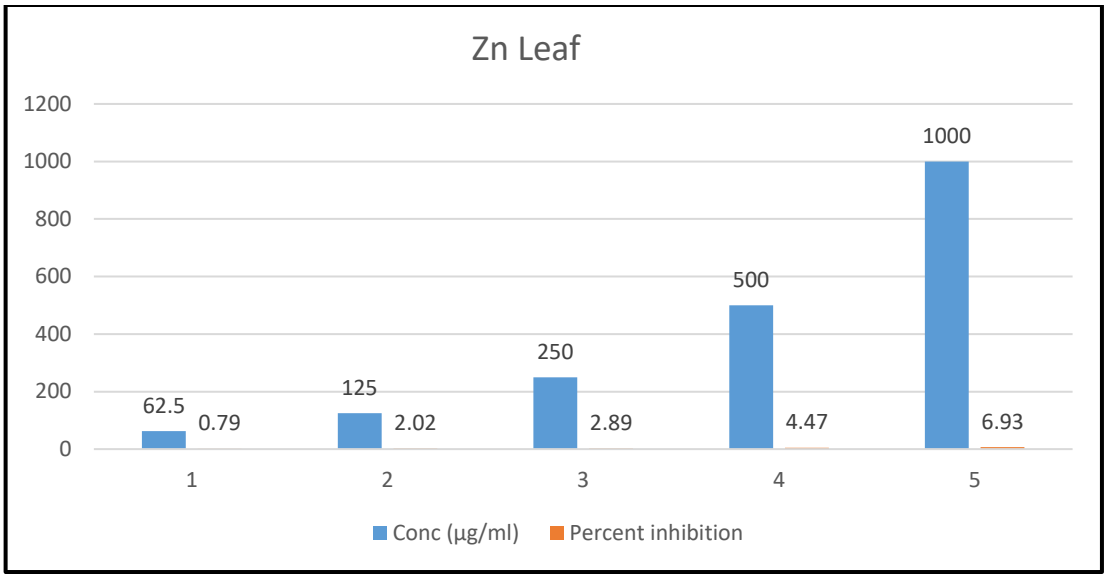

	Conc (µg/ml)	OD	Percent inhibition
Zn Leaf	**62.5**	**1.421**	**0.79**
	125	**1.407**	**2.02**
	250	**1.397**	**2.89**
	500	**1.379**	**4.47**
	1000	**1.351**	**6.93**

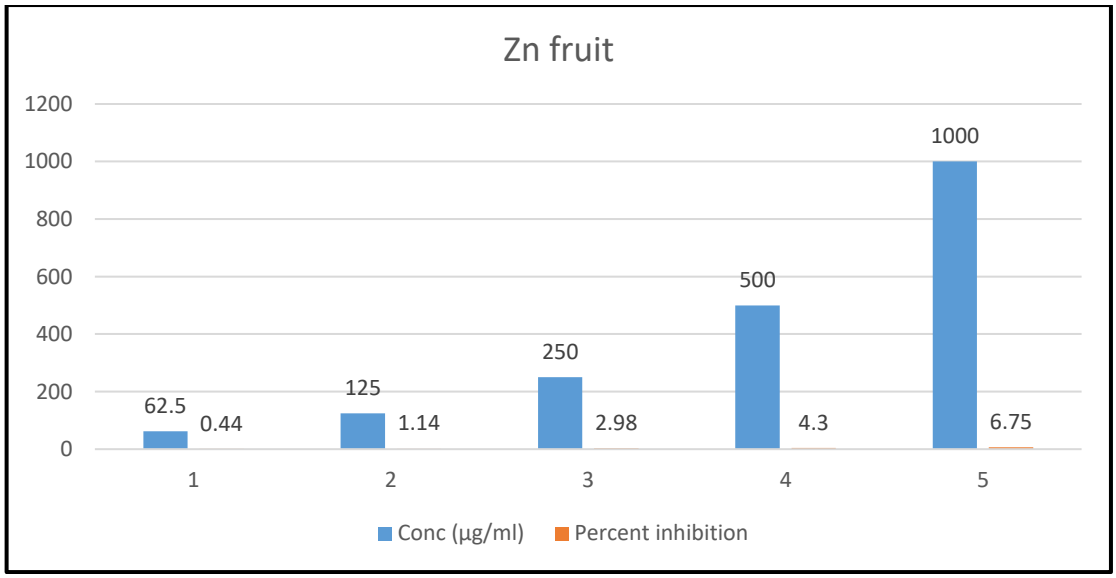

Proteinase inhibitory action

The test was performed according to the modified method. The reaction mixture (2 ml) was containing 0.06 mg trypsin, 1 ml of 20 mM Tris-HCl buffer (pH7.4) and 1ml test sample of different concentrations of different solvents. The reaction mixture was incubated at 37°C for 5 min and then 1ml of 0.8% (W/V) casein was added. The mixture was inhibited for an additional 20 min, 2 ml of 70% perchloric acid was added to terminate the reaction. Cloudy suspension was centrifuged and the absorbance of the supernatant was read at 210 nm against buffer as blank. The experiment was performed in triplicate. The percentage of inhibition of proteinase inhibitory activity was calculated.

% inhibition of denaturation = 100 × (1 – A2/A1), (3)

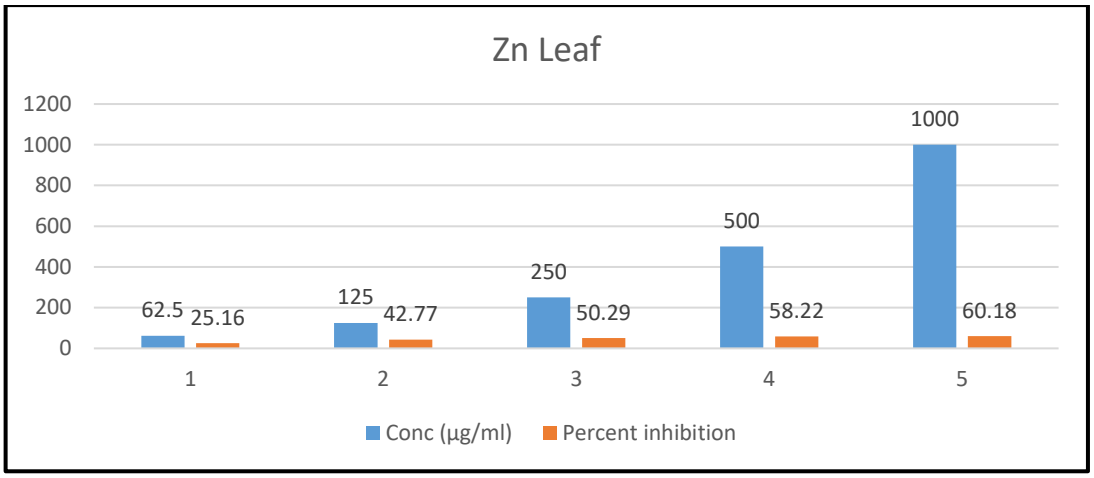

Where A1 = absorption of the control sample, and A2 = absorption of the test sample.

	Conc (µg/ml)	OD	Percent inhibition
Zn Leaf	**62.5**	**0.91**	**25.16**
	125	**1.19**	**42.77**
	250	**1.37**	**50.29**
	500	**1.63**	**58.22**
	1000	**1.71**	**60.18**

	Conc (µg/ml)	OD	Percent inhibition
CHL	**62.5**	**0.89**	**23.48**
	125	**0.96**	**29.06**
	250	**1.29**	**47.21**
	500	**1.48**	**53.99**
	1000	**1.64**	**58.48**

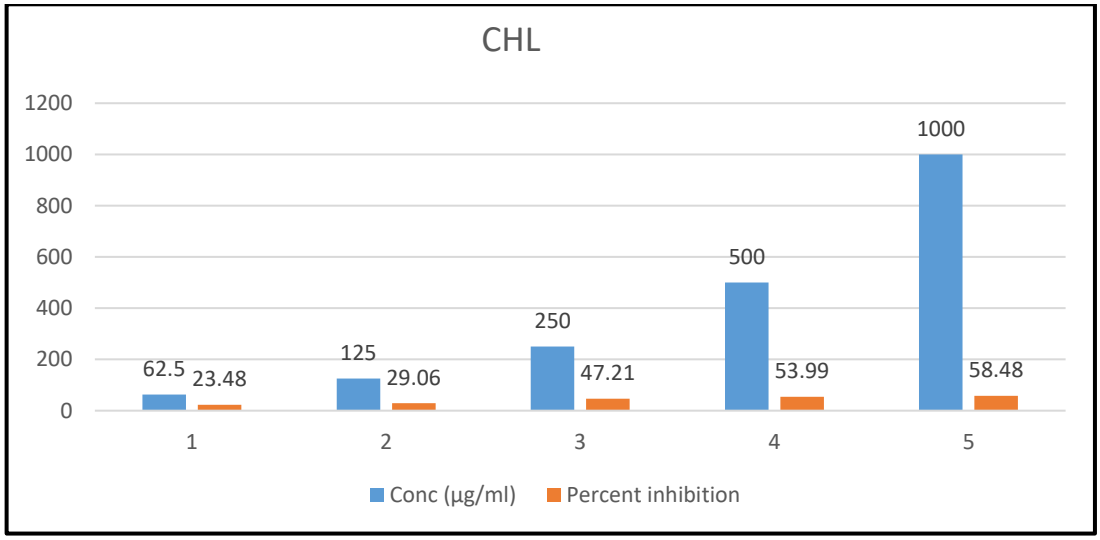

	Conc (µg/ml)	OD	Percent inhibition
CHS	**62.5**	**0.93**	**26.77**
	125	**1.25**	**45.52**
	250	**1.58**	**56.90**
	500	**1.89**	**63.97**
	1000	**2.08**	**67.26**

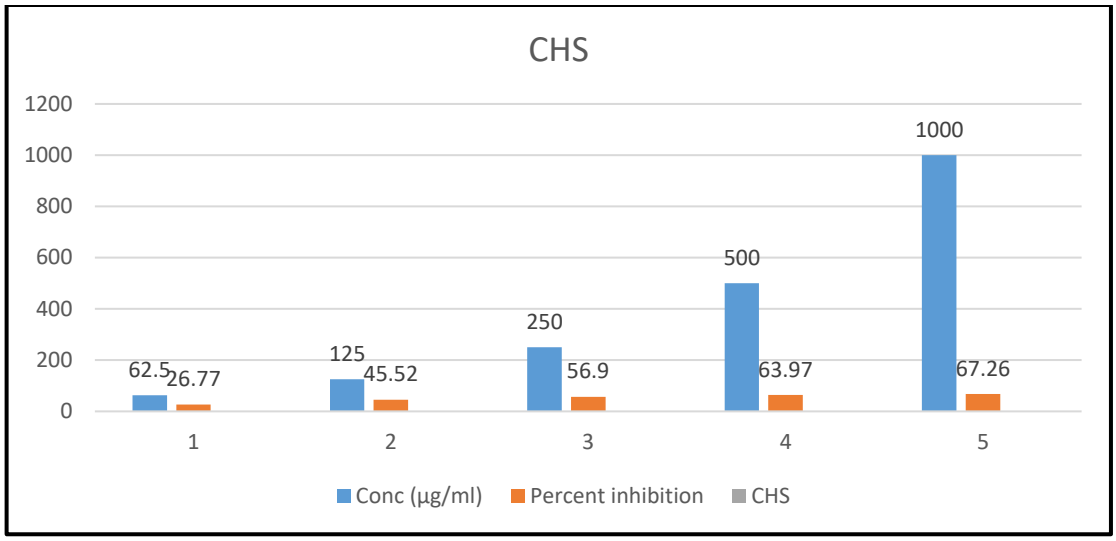

Antiproliferative activity

Evaluation of antiproliferative activities of plant extract was done by yeast *Saccharomyces cerevisiae* model.

Yeast inoculum preparation

The yeast was inoculated with sterilized potato dextrose broth and incubated at 37°C for 24 h and it was referred as seeded broth.

Determination of cell viability

Cell viability assay was performed with 2.5 mL of potato dextrose broth and 0.5 mL of yeast inoculum in four separate test tubes. In the first test tube distilled water, in second test tube quercetin (Sigma-Aldrich) as standard (1 mg/mL), in third and fourth test tubes plant extract (10 mg/mL and 5 mg/mL respectively) was added. All tubes were incubated at 37°C for 24 hours. In the above cell suspension, 0.1%methylene blue dye was added in all tubes and they were observed under low power microscope. The number of viable cells, those does not stain and look transparent with oval shape while dead cells get stained and appeared blue in color were counted in 16 chambers of hemocytometer and the average number of cell was calculated. The percentage of cell viability was calculated using the formula.

% Cytotoxicity = No. of dead cells/ No. of viable cell + No. of dead cells X 100

Compound	Concentration µg/ml	% Cytotoxicity
Zn stem	62.5	11.5
	125	18.4
	250	24.8
	500	45.9
	1000	65.2

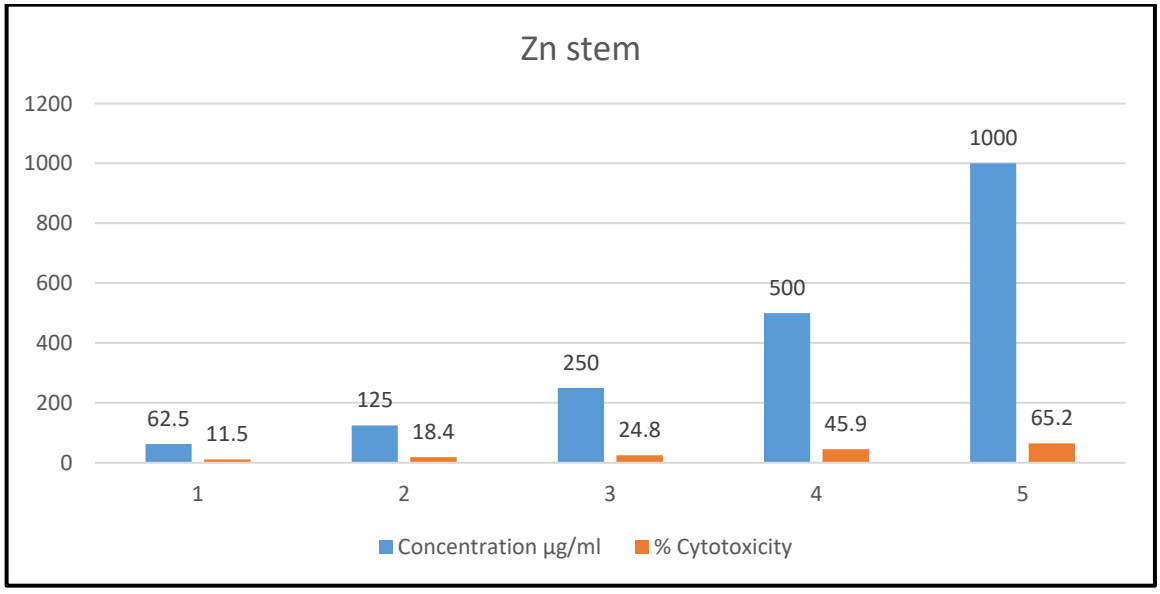

Compound	Concentration µg/ml	*% Cytotoxicity*
Zn Leaf	**62.5**	**13.2**
	125	**21.6**
	250	**42.6**
	500	**58.9**
	1000	**71.6**

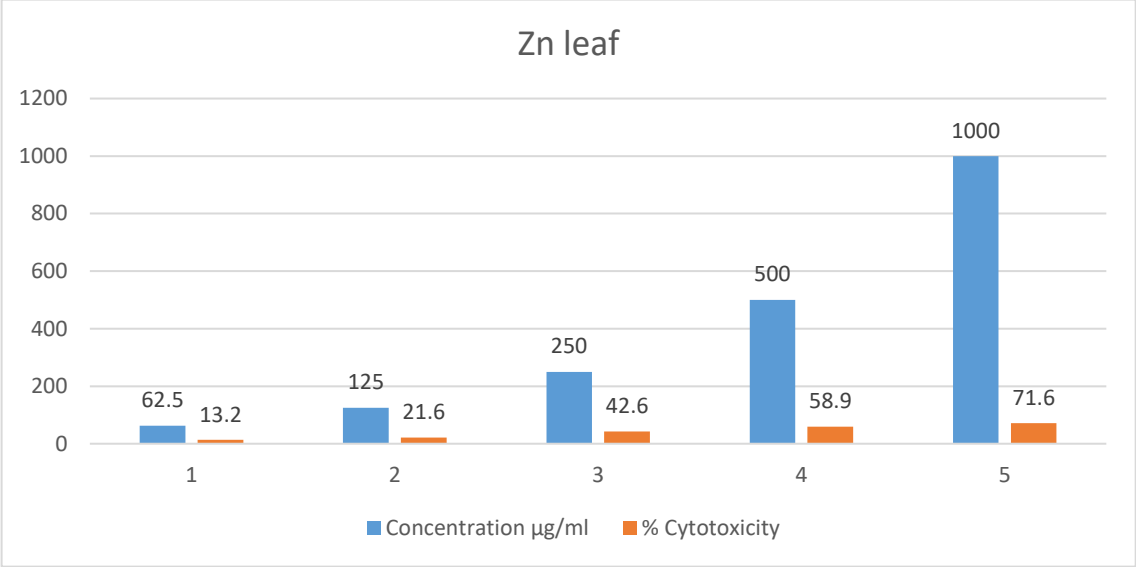

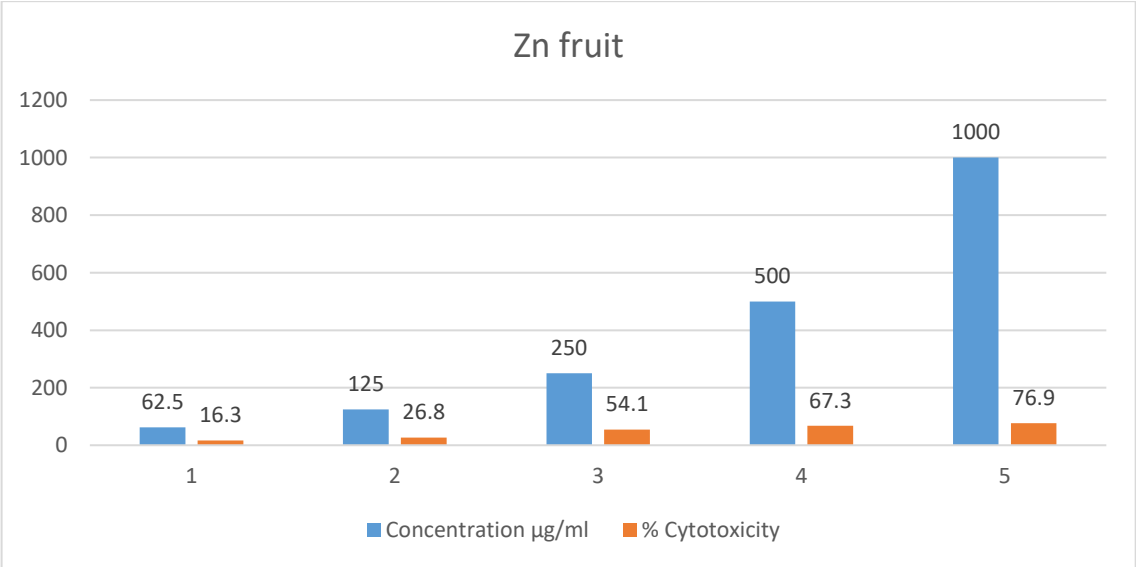

Compound	Concentration µg/ml	% Cytotoxicity
Zn fruit	**62.5**	**16.3**
	125	**26.8**
	250	**54.1**
	500	**67.3**
	1000	**76.9**

Control cells

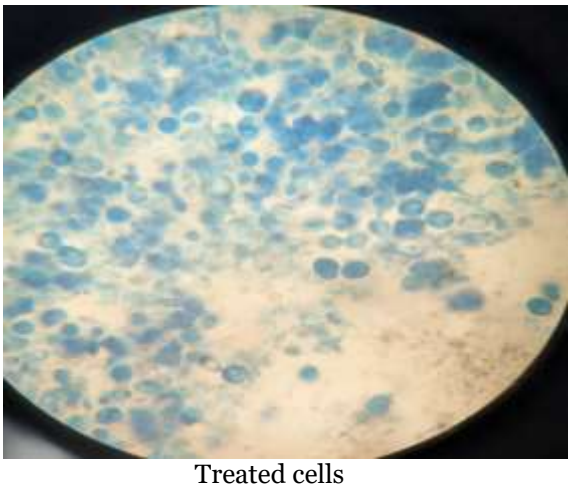

Treated cells

Conclusion

The present study shows the synthesis, Characterization of Zn NPs, these NP's acts against upon Gram positive, Gram negative bacteria & Fungi through disc diffraction methods. These Zn Nanoparticles also shows antioxidant, antiproliferation activities.

Acknowledgement

Authors are thankful to the Department of Botany of Andhra University for providing necessary facilities to conduct the studies.

References:-

1. Wang, Y., Zhao, Q., Han, N., Bai, L., Li, J., Liu, J., ... & Yang, H. (2023). "Recent advances in nanotechnology for cancer therapy and imaging." Nanoscale, 15(1), 375-389.
2. Lee, J., Kim, J., & Park, H. K. (2023). "Applications of Nanotechnology in Environmental Remediation." Environmental Science & Technology, 57(3), 1200-1218.
3. Fan Z, Lu JG. Zinc oxide nanostructures: synthesis and properties. *J Nanosci Nanotechnol.* 2005;5:1561–73. [PubMed] [Google Scholar]
4. Kalpana, V.N.; Rajeswari, V.D. A Review on Green Synthesis, Biomedical Applications, and Toxicity Studies of ZnO Nps. *Bioinorg. Chem. Appl.* 2018, *2018*, 3569758. [Google Scholar] [CrossRef] [PubMed].
5. Liu, Q., Wu, M., Li, Y., Zhou, X., & Zhu, J. J. (2023). "Recent advances in nanotechnology for diabetes management." Nano Today, 46, 101330.
6. Noman, M.T.; Amor, N.; Petru, M. Synthesis and Applications of ZnO Nanostructures (Zonss): A Review. *Crit. Rev. Solid State* 2022, *47*, 99–141. [Google Scholar] [CrossRef].
7. Jin, S.-E.; Jin, H.-E. Synthesis, Characterization, and Three-Dimensional Structure Generation of Zinc Oxide-Based Nanomedicine for Biomedical Applications. *Pharmaceutics* 2019, *11*, 575. [Google Scholar] [CrossRef] [Green Version].
8. Bahrulolum, H.; Nooraei, S.; Javanshir, N.; Tarrahimofrad, H.; Mirbagheri, V.S.; Easton, A.J.; Ahmadian, G. Green synthesis of metal nanoparticles using microorganisms and their application in the agrifood sector. J. Nanobiotechnol. 2021, 19, 86. https://doi.org/10.1186/s12951-021-00834-3
9. Somu, P.; Khanal, H.D.; Gomez, L.A.; Shim, J.J.; Lee, Y.R. Multifunctional Biogenic Al-Doped Zinc Oxide Nanostructures Synthesized Using Bioreductant Chaetomorpha Linum Extricate Exhibit Excellent Photocatalytic and Bactericidal Ability in Industrial Effluent Treatment. *Biomass Convers. Biorefin.* 2022. [Google Scholar] [CrossRef]
10. Hall, J.B.; A Dobrovolskaia, M.; Patri, A.K.; E McNeil, S. Characterization of nanoparticles for therapeutics. Nanomedicine 2007, 2, 789–803. https://doi.org/10.2217/17435889.2.6.789.
11. Zhang, D.-D.; Hu, S.; Wu, Q.; Zhao, J.-F.; Su, K.-R.; Tan, L.-Q.; Zhou, X.-Q. Construction of ZnO@mSiO_2 Antibacterial Nanocomposite for Inhibition of Microorganisms During Zea Mays Storage and Improving the Germination. *LWT-Food Sci. Technol.* 2022, *168*, 113907. [Google Scholar] [CrossRef].
12. Mendes, C.R.; Dilarri, G.; Forsan, C.F.; Sapata, V.d.M.R.; Lopes, P.R.M.; de Moraes, P.B.; Montagnolli, R.N.; Ferreira, H.; Bidoia, E.D. Antibacterial action and target mechanisms of zinc oxide nanoparticles against bacterial pathogens. Sci. Rep. 2022, 12, 2658. https://doi.org/10.1038/s41598-022-06657-y
13. Abomuti, M.A.; Danish, E.Y.; Firoz, A.; Hasan, N.; Malik, M.A. Green Synthesis of Zinc Oxide Nanoparticles Using Salvia officinalis Leaf Extract and Their Photocatalytic and Antifungal Activities. Biology 2021, 10, 1075. https://doi.org/10.3390/bi- ology10111075.

14. Xu, M.-N.; Li, L.; Pan, W.; Zheng, H.-X.; Wang, M.-L.; Peng, X.-M.; Dai, S.-Q.; Tang, Y.-M.; Zeng, K.; Huang, X.-W. Zinc Oxide Nanoparticles Prime a Protective Immune Response in Galleria mellonella to Defend Against Candida albicans. Front. Microbiol. 2021, 12. https://doi.org/10.3389/fmicb.2021.766138.
15. Kalaimurugan, D.; Lalitha, K.; Durairaj, K.; Sivasankar, P.; Park, S.; Nithya, K.; Shivakumar, M.S.; Liu, W.-C.; Bal- amuralikrishnan, B.; Venkatesan, S. Biogenic synthesis of ZnO nanoparticles mediated from Borassus flabellifer (Linn): An- tioxidant, antimicrobial activity against clinical pathogens, and photocatalytic degradation activity with molecular model- ing. Environ. Sci. Pollut. Res. 2022, in press
16. Asif, N.; Fatima, S.; Aziz, N.; Shehzadi; Zaki, A.; Fatma, T. Biofabrication and characterization of cyanobacteria derived ZnO NPs for their bioactivity comparison with commercial chemically synthesized nanoparticles. Bioorganic Chem. 2021, 113, 104999. https://doi.org/10.1016/j.bioorg.2021.104999.
17. Alarifi, Saud, et al. "Fungi-assisted zinc nanoparticles synthesis and their characterization." Journal of King Saud University-Science 31.2 (2019): 353-357